The limiting effect of breaking in strongly nonlinear waves on intermediate water depth, with emphasis on the kinematics

John Grue, Jostein Kolaas and Atle Jensen
Mechanics Division, Department of Mathematics, University of Oslo, Norway

Background and motivation. There is currently a great interest in the production of clean energy from wind at sea. Such production in the offshore environment benefits from a wind that is stronger and more even than over land. Moreover, larger areas are available for this type of energy source where the relative energy density is small. The wind turbines that recently have been installed offshore on, e.g., Horns Rev, have a production capacity of 2.1 MW. However, cost reduction plans of offshore wind turbines have enforced the industry to develop new turbines with even larger production capacity, up to 6-7 MW. The offshore wind turbines are commonly placed on circular piles standing on the sea bottom. The water depth at actual locations is in the range 12–24 m on Sheringham Shoal (developed) and 15–36 m on Dogger Bank (planned). The very tall and massive geometries are exposed to the wind and wave loads, where in this paper the latter is addressed. We shall specifically address the kinematics of the strongest possible waves on finite water depth.

Regarding the range of the wave periods, it is considered from an engineering point of view, that waves up to 12 seconds may be the strongest and give the most energetic loads on the structures. The corresponding nondimensional period is in the range $T\sqrt{g/h} \sim 11 - 6$ for water depth in the range $h \sim 12 - 36$ m (g acceleration of gravity) corresponding to water waves on intermediate depth. This means that potentially very long waves such as tsunamis and their by products such as solitary waves or periodic cnoidal waves may not be of interest. Industries working on offshore wind farm developments have requested more documentation of the kinematics of very strong waves on intermediate water depth, particularly the effect of breaking. This is investigated here. We are particularly addressing two points:

1) How are the velocities in the strongest possible water waves on finite depth?

2) How do weak and strong breaking alter the kinematics?

Experiments on breaking waves. Periodic waves of largest possible elevation propagating along a fluid layer of constant depth h are characterized by the period T and height H. Two slightly different wave periods of $T\sqrt{g/h} = 8.8$ and 11.7 investigated here correspond to the practical range of interest for offshore wind turbine applications.

The wave paddle amplitude is gradually increased from small to large excursion, beyond the level where breaking starts. Incipient wave breaking occurs about ten water depths from the wave maker. The breaking point moves towards the wave maker according to the increasing strength of the wave generation. The waves radiating out reach a saturation of the wave height corresponding to a maximum value.

Waves of periods $T\sqrt{g/h} = 8.8$ and 11.7 have a maximum height far away from the generation site of $H/h \simeq 0.49$, see Nelson (1994, figure 1) and is also obtained in the present experiments; longer waves than measured here have H up to $0.55h$. The periodic far field waves are nonbreaking. Still stronger wave paddle motion reduces the elevation in the far field because of the stronger breaking taking place close to the wave

maker. The wave breaking process and the finite excursion of the wave maker generate additional short higher harmonic waves riding on top of the dominant motion.

Strongly and moderately breaking waves close to the wave paddle are measured by Particle Tracking Velocimetry (PTV) (for experimental arrangements, see below). Several series of wave breaking measurements, each including 24 wave crests, are recorded 10 water depths from the wave maker. Figure 1 shows three among the most violent waves. The breaking is visible in the form of a band corresponding to a turbulent region indicated by light color in the figure, between the wave surface and a smooth region below, indicated by dark color. Fluid velocities are obtained in the smooth flow. We have not been able to obtain velocities in the turbulent region.

The strongest wave making amplitude gives a maximum wave height (close to the wave maker) of $0.56h$, average height of $0.51h$ and standard deviation of 3.7 % (figure 1a). Velocities below one of the strongest crests are up to $0.6\sqrt{gh}$ (8.5 s$< t <$9.6 s). The wave profile is somewhat asymmetrical (figure 2). The ensemble of velocity profiles below the 24 crests shows that $u/\sqrt{gh} = 0.72$ at maximum and that $u/\sqrt{gh} = 0.6 \pm 0.05$ is a typical picture of the wave induced velocities below all of the crests (figure 3a). The strongly breaking waves induce strong oscillations of large scale of the velocities, particularly in the back of the wave (figure 3b). The significant higher harmonic content of the wave induced motion is caused by the wave overturning and dominate the usual nonlinearities (finite elevation, square term in the Bernoulli equation).

Moderately breaking waves (weaker wave making amplitude) have $H = 0.63h$ at maximum and average height of $0.58h$ (figure 1c). The ensemble of velocity profiles below the 24 crests shows that $u/\sqrt{gh} = 0.6$ at maximum and that $u/\sqrt{gh} = 0.5 \pm 0.05$ is a typical picture of the velocity maxima of all of the crests.

Accelerations. The horizontal acceleration of the strongly breaking wave fields are visualized by evaluating the vertical average of the velocity arrows, at each horizontal position and time of the PTV images, and then taking the time derivative, i.e. we evaluate $\dot{\bar{u}}$, where a bar denotes vertical average. This vertical average is evaluated where the velocity arrows are measured, i.e. in the smooth flow indicated by the dark color in figure 1. The acceleration in the strongly breaking waves is in the range $-0.2 \sim< \dot{\bar{u}}/g <\sim 0.29$, i.e. almost up to 30 per cent of the acceleration of gravity (figure 4). The results moreover illustrate the higher harmonic components in the strongly breaking waves. The measurements of the horizontal acceleration may be used as input to force calculations using an inertia based force formulation valid for slender geometries, e.g. Morison's equation.

Far field waves. The periodic wave train far away from the wave maker reaches a steady state where small higher harmonic free waves – generated by combination of breaking or local steepening about one wave length away from the wave maker, as well as by the finite excursion of the wave maker – ride on top of the dominant wave motion. It is assumed that this scenario is representative for the real waves on the ocean. As for the main wave, the higher harmonic waves become saturated in amplitude due to breaking. The higher harmonic waves alter the crest and trough levels as well as the kinematics of the wave field. For the wave train with $T\sqrt{g/h} = 8.75$ and $H/h = 0.49$ we find that the horizontal fluid is $u/\sqrt{gh} = 0.5$ at maximum. This is 16 per cent higher than fully nonlinear calculations by Fenton's method (1988) for the same wave,

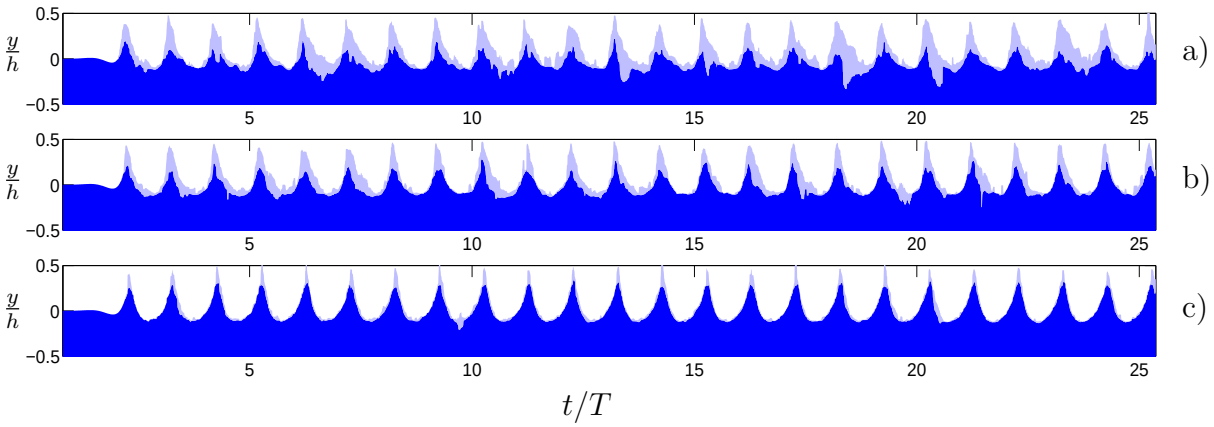

Figure 1: PTV recordings of breaking waves at 2.08 m. $T\sqrt{g/h} = 8.75$. 24 crests in each series. Smooth flow (dark). Breaking turbulent flow (light). Wave maker amplitude: a) $\xi_0/h = 0.3697$, b) $\xi_0/h = 0.3287$, c) $\xi_0/h = 0.2876$.

assuming periodic waves without any parasittic effects – we have used 20 terms in these calculations. In the leading part of this wave train, before the higher harmonic waves arrive at the measurement position, we have an almost perfect match between the experimental wave and the calculation. With $T\sqrt{g/h} = 11.7$, $H/h = 0.48$, the horizontal velocity is up to $u/\sqrt{gh} = 0.4$ in the experiments. Nonlinear calculations give about the same kinematics; the nominal crest and trough values are somewhat larger in the theoretical wave compared to experiment. Results of the far field waves are presented in Grue et al. (2014).

Experimental arrangements. The elevation and kinematics are obtained experimentally by PTV. Waves generated by a vertical piston at one end of a wave tank, 25 m long, 0.5 m wide and water depth of 0.2 m, are recorded long before any reflection appears from the beach at the other end of the tank. Field Of Views (FOVs) of 0.2 by 0.2 m have resolution of 1024 by 1024 pixels. The number of frames per second is 200 for breaking waves and 1500 for nonbreaking waves; 6000 frames are recorded in each series.

Acknowledgement. This research was funded by the Research Council of Norway through NFR191204/V30 “Wave-current-body interaction”.

References

J. D. Fenton (1988), The numerical solution of steady water wave problems. Computers & Geosciences 14(3), 357-368.

J. Grue, J. Kolaas and A. Jensen (2014), Velocity fields in breaking-limited waves on finite depth. Eur. J. Mech. B/Fluids (submitted).

R. C. Nelson (1994), Depth limited design wave heights in very flat regions. Coastal Engineering 23, 43-59.

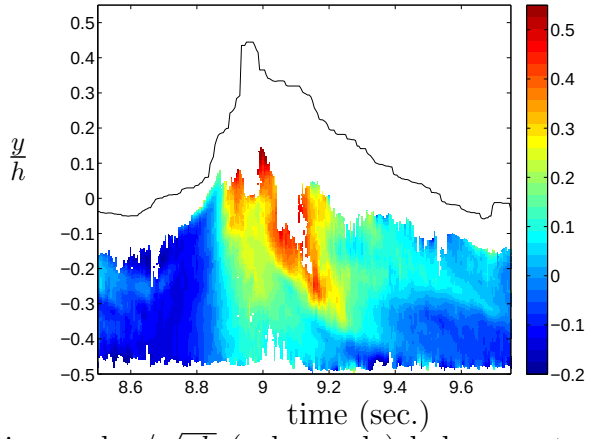

Figure 2: Elevation and $u/\sqrt{gh}$ (color scale) below crest number 6 in figure 1a (8.6 s$< t <$ 9.75 s).

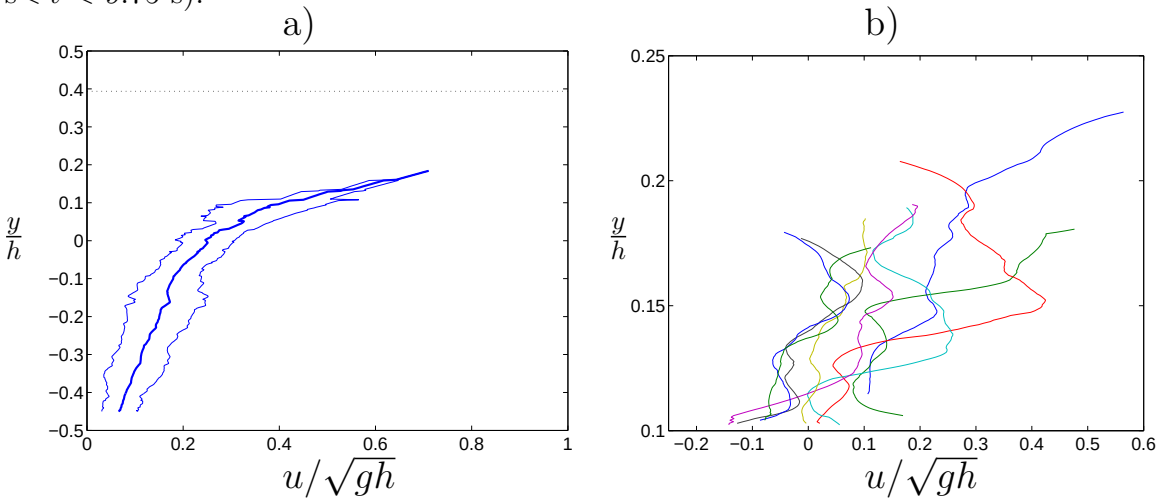

Figure 3: a) Ensemble average (thick line) and standard deviation (thin lines) of all velocity profiles $u/\sqrt{gh}$ vs. y/h below the 24 crests in figure 1a. b) Horizontal velocity profiles with $\Delta t\sqrt{g/h} = 1.75$ in back part of the wave in figure 2.

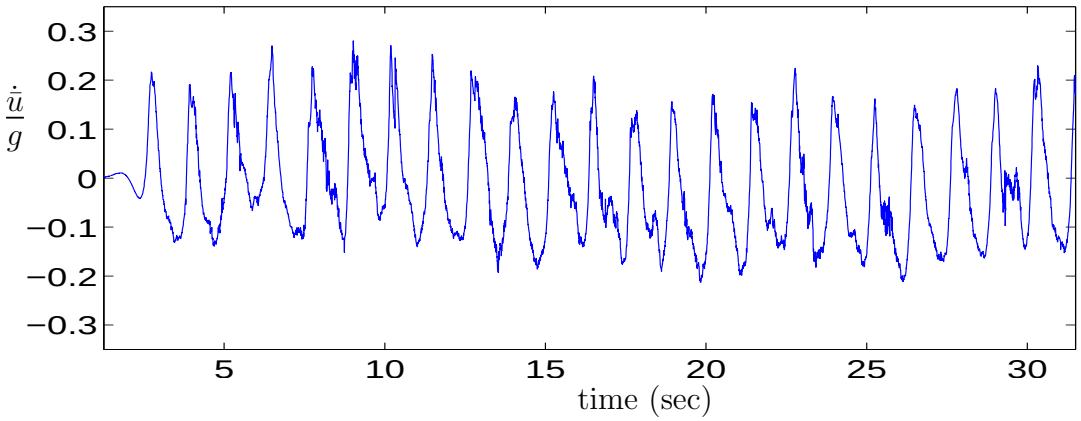

Figure 4: Horizontal acceleration (vertical average) $\frac{\dot{u}}{g}$ vs. time for the strongly breaking waves in figure 1a. Wave motion from right to left (negative acceleration in the front of the wave).